Aggregation and Motor Neuron Toxicity of an ALS-Linked SOD1 Mutant Independent from Wild-Type SOD1

Lucie I. Bruijn,* Megan K. Houseweart, Shinsuke Kato, Karen L. Anderson, Scott D. Anderson, Eisaku Ohama, Andrew G. Reaume, Rick W. Scott, Don W. Cleveland†

Analysis of transgenic mice expressing familial amyotrophic lateral sclerosis (ALS)–linked mutations in the enzyme superoxide dismutase (SOD1) have shown that motor neuron death arises from a mutant-mediated toxic property or properties. In testing the disease mechanism, both elimination and elevation of wild-type SOD1 were found to have no effect on mutant-mediated disease, which demonstrates that the use of SOD mimetics is unlikely to be an effective therapy and raises the question of whether toxicity arises from superoxide-mediated oxidative stress. Aggregates containing SOD1 were common to disease caused by different mutants, implying that coaggregation of an unidentified essential component or components or aberrant catalysis by misfolded mutants underlies a portion of mutant-mediated toxicity.

After the discovery (*1*) that dominant missense mutations in Cu/Zn superoxide dismutase (SOD1) were the primary cause of 15 to 20% of familial ALS cases, experiments with transgenic mice expressing ALS-linked mutations showed that selective motor neuron degeneration arises from toxic properties of the ubiquitously expressed mutant enzymes (*2–5*). This has fueled proposals that (i) mutant SOD1s have an altered substrate affinity that leads to high levels of toxic reaction products (*6–8*); (ii) the reduced SOD activity arising from unstable or imperfectly folded enzymes causes toxic oxidative stress through an imbalance in oxidative defenses (*9*, *10*), which in turn may exacerbate aberrant catalysis; or (iii) poorly or unstably folded mutants mitigate SOD1-containing aggregates that are toxic to motor neurons (*5*, *11*).

To test these hypotheses, the influence of wild-type SOD1 polypeptide and activity levels on the onset and progression of SOD1 mutant toxicity was determined by eliminating or elevating wild-type SOD1 in mice developing motor neuron disease due to expression of an ALS-linked mutant with glycine substituted to arginine at position 85 ($SOD1^{G85R}$). Because in vivo the $SOD1^{G85R}$ mutant polypeptide appears to retain only about 10% of the activity of the wild-type SOD1 (at least when expressed in yeast) (*12*) and disease arises with low levels of the mutant protein (*5*), neither SOD1 activity nor polypeptide levels are markedly elevated in the $SOD1^{G85R}$ animals.

$SOD1^{G85R}$ mice were mated to mice expressing wild-type human SOD1 at six times the level of endogenous mouse SOD1 (*13*). In addition, a two-stage breeding strategy (*13*) was used with mice carrying a targeted deletion of the endogenous SOD1 gene (*14*) to generate mice expressing $SOD1^{G85R}$ in the absence of endogenous SOD1, along with littermates with one or both endogenous SOD1 alleles. Total spinal cord extracts from two animals from each genotype were immunoblotted with an antipeptide antibody (*15*) that reacts exclusively with human, but not mouse, SOD1. Neither a sixfold increase in wild-type SOD1 (Fig. 1A) nor its complete elimination (Fig. 1B) affected the accumulated levels of mutant $SOD1^{G85R}$ protein. Thus, despite a decreased stability of $SOD1^{G85R}$ relative to wild-type SOD1 in these mice (*5*), the wild-type protein did not stabilize mutant SOD1. Moreover, the presence of $SOD1^{G85R}$ had no effect on the level (Fig. 1A) or the activity of wild-type SOD1.

Survival plots comparing transgenic mice expressing both $SOD1^{G85R}$ and wild-type human SOD1 (Fig. 2A, solid squares, $n = 20$) or $SOD1^{G85R}$ alone (Fig. 2A, open squares, $n = 14$) indicated that increasing wild-type SOD1 activity and polypeptide level had no beneficial effect. Age distributions at end-stage disease were indistinguishable (with the exception that a small fraction of mice with normal SOD1 levels survived up to 20 days longer). There were no differences in age of disease onset, and duration after onset was also constant (a median of 18 days for both genotypes). Similarly, no differences in age at end-stage disease could be seen among mice expressing $SOD1^{G85R}$ in the presence of normal levels of mouse SOD1 (Fig. 2B, triangles, $n = 5$) when levels of mouse SOD1 were reduced to 50% of normal levels (Fig. 2B, open circles, $n = 10$) or in the complete absence of endogenous mouse SOD1 (Fig. 2B, solid circles, $n = 5$).

A prominent pathology found in all mouse lines that develop ALS-like disease from expressing $SOD1^{G85R}$ is neuronal and astrocytic inclusions that appear in the $SOD1^{G85R}$ mice before clinical signs, increase markedly

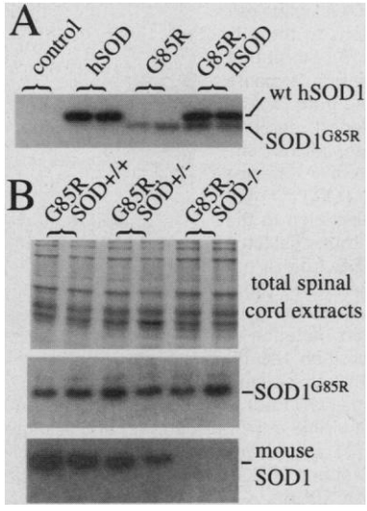

Fig. 1. The presence or absence of wild-type protein does not affect the stability of mutant protein. **(A)** Levels of wild-type human SOD1 or mutant $SOD1^{G85R}$ determined by immunoblotting spinal cord extracts from normal mice (control), transgenic mice expressing wild-type human SOD1 to six times the level of endogenous mouse SOD1 (hSOD), transgenic mice expressing $SOD1^{G85R}$ (G85R), or mice carrying both the hSOD1 and $SOD1^{G85R}$ transgenes (G85R, hSOD). Each pair of slots represents analyses from duplicate animals. Human SOD1 was detected with a peptide antibody specific for human, but not mouse, SOD1 (*5*). **(B)** Total spinal cord extracts from mice transgenic for $SOD1^{G85R}$ and carrying both endogenous SOD1 alleles (G85R, $SOD^{+/+}$) or carrying a deletion of one (G85R, $SOD^{+/-}$) or both (G85R, $SOD^{-/-}$) endogenous SOD1 alleles. Top panel, Extract proteins detected with Coomassie blue; middle and bottom panels, immunoblots with antibodies specific for human SOD1 (middle) or mouse SOD1 (bottom) (*5*, *25*).

L. I. Bruijn, M. K. Houseweart, K. L. Anderson, S. D. Anderson, D. W. Cleveland, Ludwig Institute for Cancer Research and Departments of Medicine and Neuroscience, University of California, La Jolla, CA 92093, USA. S. Kato and E. Ohama, Department of Neuropathology, Institute of Neurological Sciences, Faculty of Medicine, Tottori University, Yonago 683, Japan. A. G. Reaume and R. W. Scott, Cephalon, 145 Brandywine Parkway, Westchester, PA 19380, USA.

*Present address: Pharmaceutical Research Institute, Bristol-Myers Squibb, Wallingford, CT 06492–7660, USA.

†To whom correspondence should be addressed. E-mail: dcleveland@ucsd.edu

in abundance during disease progression (*5*), and are highly immunoreactive for SOD1 that is concentrated either at the periphery of the inclusion or throughout it (Fig. 3B, arrowheads) or more diffusely localized in aggregates (Fig. 3B, arrows), many of which (for example, Fig. 3B, lower right arrow) are not identified by conventional histological stains (Fig. 3A). Examination of mice expressing other SOD1 mutants revealed that this is a common pathology of SOD1 mutant–mediated ALS in mice, because diffuse aggregates that are strongly immunoreactive for SOD1 (Fig. 3D, arrows) and SOD1-containing inclusions (Fig. 3D, arrowheads) observable by conventional histology are also found in both astrocytes and neurons of lines expressing high levels of $SOD1^{G93A}$ (Fig. 3C), as well as one line expressing low levels of $SOD1^{G93A}$ (*16*) and in neurons in several $SOD1^{G37R}$ lines (*17*). Neither type of SOD1 aggregate was found at any age in mice expressing wild-type human SOD1. Similar SOD1-containing aggregates have also been reported for some human sporadic (*18–20*) and familial (*21–24*) ALS cases, including a familial ALS patient with a 2–base pair deletion at codon 126 of SOD1 (Fig. 3, E and F). Because this latter mutation truncates the final 27 amino acids of SOD1 (*23*), strong immunostaining of these aggregates with an antipeptide antibody against SOD1 amino acids 125 through 137 (*25*) showed that wild-type SOD1 is an apparently prominent component of these aggregates (Fig. 3F).

To examine whether wild-type SOD1 exacerbated the aggregates, pathology arising during disease progression was determined in $SOD1^{G85R}$ mice with varying levels of wild-type SOD1. Before the onset of symptoms (at ages up to 7.5 months), there were no SOD1-positive inclusions or reactive astrocytes in spinal cords from the any of the mice and no axonal degeneration in dorsal or ventral roots. A 70% loss of large (>5 μm) caliber motor axons in the L5 ventral root was seen at end-stage disease in $SOD1^{G85R}$ transgenic mice independent of the wild-type SOD1 content, whereas the small-caliber axons were almost completely spared (Table 1). Similarly, in all genotypes the numbers of

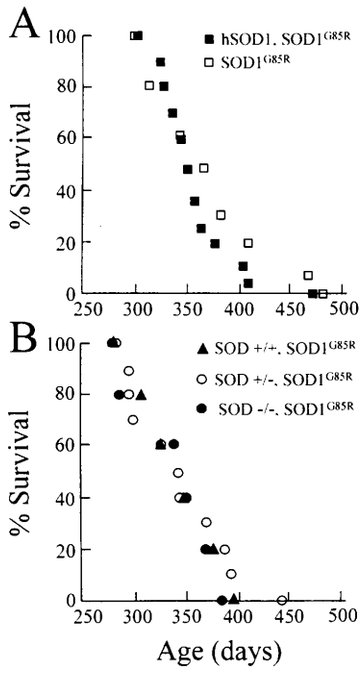

Fig. 2. Disease onset and progression mediated by $SOD1^{G85R}$ are independent of wild-type SOD1 protein or activity levels. (**A**) Survival plots of $SOD1^{G85R}$ transgenic mice (■) with or (□) without a human wild-type SOD1 transgene to elevate wild-type SOD1 levels to six times the normal amount. (**B**) Survival plots of mice with the $SOD1^{G85R}$ transgene and (▲) both endogenous mouse SOD1 genes or (○) heterozygously or (●) homozygously deleted for endogenous mouse SOD1.

Table 1. Surviving large and small motor axons at end-stage disease in the L5 ventral roots of mice with normal, reduced, or elevated levels of wild-type SOD1. Statistical tests (analysis of variance, $P = 0.826$) revealed no significant diference between the numbers of large surviving axons in G85R; G85R, $SOD^{+/-}$; G85R, $SOD^{-/-}$; and G85R, hSOD1 mice. For all genotypes, three mice were analyzed, except that marked with an asterisk, for which two animals were measured.

Surviving axons	Wild-type mice (12 months)	G85R	G85R, $SOD^{+/-}$	G85R, $SOD^{-/-}$*	G85R, hSOD1
Large (>5 μm)	730 ± 12	188 ± 13	145 ± 51	221 ± 138	183 ± 18
Small (≤ 5μm)	304 ± 23	295 ± 24	293 ± 5	234 ± 2	295 ± 11

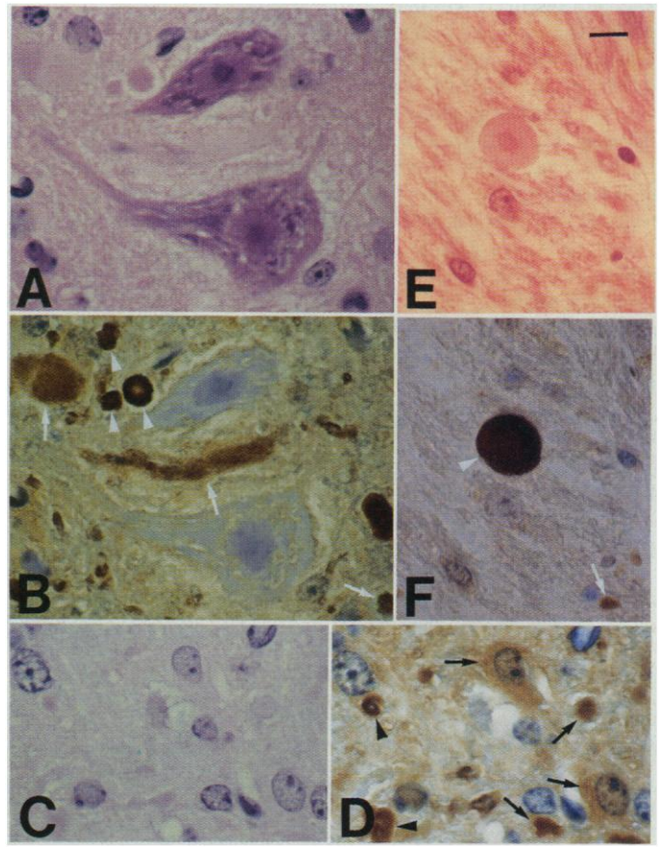

Fig. 3. Inclusions that are strongly immunoreactive with SOD1 antibodies are common features in transgenic mice expressing $SOD1^{G93A}$, $SOD1^{G85R}$, and $SOD1^{G37R}$ and resemble those seen in human patients with familial ALS. (**A**) Hemotoxylin and eosin (H&E) staining of the ventral portion of a spinal cord from an end-stage mouse expressing mutant $SOD1^{G85R}$. (**B**) The identical section as in (A) (*35*), reacted with an antibody recognizing both mouse and human mutant SOD1. (**C** and **D**) A similar pair of sections to those in (A) and (B), except that they are from a mouse (obtained from Jackson Laboratories) developing motor neuron disease from expressing mutant $SOD1^{G93A}$ (*2*). (**E**) An inclusion in the spinal cord, detected with H&E, from a patient who died from disease mediated by a frameshift mutation at SOD1 position 126. (**F**) The identical section as in (E) (*35*), reacted with an antipeptide antibody that recognizes human wild-type SOD1 but not the truncated mutant. Arrowheads in (B), (D), and (F) point to inclusions that are visible in (A), (C), and (E) and are intensely immunoreactive to SOD1 antibodies. Arrows in (B), (D), and (F) point to SOD1 immunoreactive aggregates that appear to contain less dense accumulations of SOD1, which may be the precursors of the more intensely stained aggregates. Scale bar, 10 μm.

motor and sensory axons degenerating at the end stage were comparable, as were the numbers of aggregates in motor neurons and astrocytes (Fig. 4A), each of which was immunoreactive for SOD1 (Fig. 4B, arrowheads), as well as more diffuse SOD1-containing aggregates (Fig. 4B, arrows).

Thus, changing the levels of wild-type SOD1 polypeptides and activity between none and six times the normal level of SOD1 did not affect the pathology, onset, or progression of disease mediated by familial ALS mutant $SOD1^{G85R}$. These findings are incompatible with several proposed toxic properties of the mutants and bear directly on possible therapeutic strategies.

First, contrary to earlier in vitro evidence (*6*, *7*, *26*, *27*), these results showed that motor neuron degeneration almost certainly did not arise from more efficient use of either peroxynitrite or H_2O_2. Peroxynitrite production [proposed to form through the spontaneous reaction of nitric oxide with superoxide (*6*)] should be substantially elevated by the absence of wild-type SOD1 and probably lowered by a more rapid removal of superoxide in mice with a sixfold elevation of wild-type SOD1, thereby accelerating or slowing disease, respectively. This was clearly not the case for mutant $SOD1^{G85R}$. When coupled with the absence of biochemically detectable protein nitration in $SOD1^{G37R}$ (*28*) and $SOD1^{G93A}$ (*29*) mice, it seems unlikely that such enzyme-mediated nitration is a key toxic property, despite apparent increases in nitration that have been reported using immunocytochemistry in some cases of familial and sporadic ALS (*19*, *30*) and in $SOD1^{G93A}$ mice (*29*). Similarly, although we cannot directly measure the levels of intracellular H_2O_2, one might predict an elevation or lowering of H_2O_2 caused by increasing or decreasing levels of wild-type SOD1. This in turn would accelerate or slow disease were the mutant to use H_2O_2 more efficiently than the wild type. On the other hand, it may be that the H_2O_2 produced in the active site from superoxide is the preferred substrate for aberrant catalysis. A sixfold molar excess of wild-type SOD1 would obviously reduce the access of the mutant to superoxide (through competition or by accelerated catalytic destruction of it, or both), whereas elimination of wild-type SOD1 would strongly enhance it. Both would predict changes in the rate of damage. But our evidence, along with the absence of evidence for predicted damaged products in $SOD1^{G37R}$ (*28*) and $SOD1^{G93A}$ (*29*) mice and in vitro evidence questioning whether the mutants do use H_2O_2 as a substrate (*31*), showed that this too was not the case.

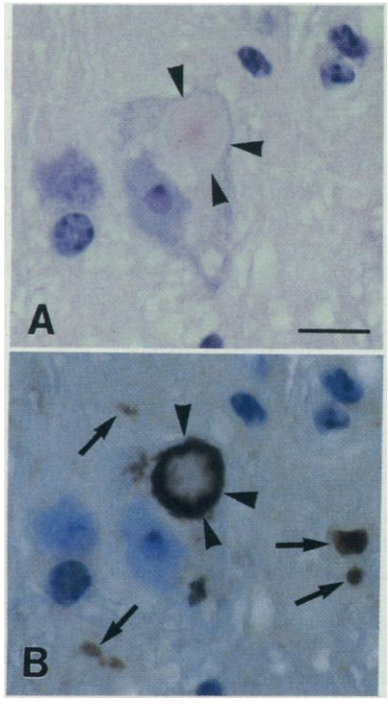

Fig. 4. SOD1-immunoreactive aggregates form in the absence of endogenous mouse SOD1. **(A)** H&E staining of the ventral portion of a spinal cord from an end-stage mouse expressing mutant $SOD1^{G85R}$ and deleted in both endogenous SOD1 alleles. **(B)** The identical section as in (A) (*35*), reacted with an antibody recognizing both mouse and human mutant SOD1. The central arrowheads in (A) and (B) point to an inclusion that reveals a halo of intense immunoreactivity to SOD1 antibodies. Arrows point to inclusions that have uniform SOD1 immunoreactivity and are not readily identifiable with H&E. Scale bar, 10 μm.

Second, the fact that disease was not accelerated in the complete absence of wild-type SOD1 argues directly against the hypothesis (*9*, *32*) that toxicity arises even in part from a reduction in normal SOD1 activity. Third, although we show that wild-type SOD1 was a component of aggregates in human disease, the wild-type protein was not required for aggregation, either for stabilizing the mutant or for contributing to aggregates nucleated by mutant SOD1.

Finally, the failure of increased SOD1 activity to ameliorate disease argues strongly against potential therapeutic attempts to slow disease by increasing superoxide scavenging activities using SOD1 mimetics. Indeed, the absence of influence of SOD1 activity on mutant toxicity challenges the idea that toxicity derives from (or is even linked to) oxidative stress arising from superoxide. Rather, mutant SOD1–containing aggregates that coincide with disease onset and that increase in abundance as disease progresses were found to be common to disease caused by different mutants. However, this cannot be the whole story concerning toxicity, because mutant-mediated defects (including a selective slowing of some cargoes of slow axonal transport) are seen at least 5 months before the appearance of aggregates (*33*); and a mating experiment strategy similar to that used here has proven that in the absence of neurofilaments, $SOD1^{G85R}$ mediates disease with a substantially delayed onset (*34*) and a markedly reduced frequency of SOD1-containing aggregates (*33*). Nevertheless, the present efforts support the idea that one aspect of toxicity may arise through an as-yet-unidentified chemistry mediated by the misfolded aggregated mutants or through loss by coprecipitation of an essential component or components.

References and Notes

1. D. R. Rosen *et al.*, *Nature* **362**, 59 (1993).
2. M. E. Gurney *et al.*, *Science* **264**, 1772 (1994).
3. M. E. Ripps, G. W. Huntley, P. R. Hof, J. H. Morrison, J. W. Gordon, *Proc. Natl. Acad. Sci. U.S.A.* **92**, 689 (1995).
4. P. C. Wong *et al.*, *Neuron* **14**, 1105 (1995).
5. L. I. Bruijn *et al.*, *ibid.* **18**, 327 (1997).
6. J. S. Beckman, M. Carson, C. D. Smith, W. H. Koppenol, *Nature* **364**, 584 (1993).
7. M. Wiedau-Pazos *et al.*, *Science* **271**, 515 (1996).
8. S. I. Liochev, L. L. Chen, R. A. Hallewell, I. Fridovich, *Arch. Biochem. Biophys.* **346**, 263 (1997).
9. H.-X. Deng *et al.*, *Science* **261**, 1047 (1993).
10. R. Orrell, J. Belleroche, S. Marklund, F. Bowe, R. Hallewell, *Nature* **274**, 504 (1995).
11. H. D. Durham, J. Roy, L. Dong, D. A. Figlewicz, *J. Neuropathol. Exp. Neurol.* **56**, 52 (1997).
12. L. B. Corson, J. Strain, V. C. Culotta, D. W. Cleveland, *Proc. Natl. Acad. Sci. U.S.A.* **95**, 6361 (1998).
13. $SOD1^{G85R}$ mice (line 148) (*5*) were bred to mice overexpressing human wild-type SOD1 (hSOD1, line 30) (*4*) to six times the level of endogenous SOD1. $SOD1^{G85R}$ mice were bred with mice heterozygous for SOD1 deletion ($SOD1^{+/-}$) to generate $SOD1^{G85R}$, $SOD1^{+/-}$ mice, which were then bred with $SOD1^{+/-}$ mice to generate, in the same litters, $SOD1^{G85R}$ mice with zero, one, or two copies of the endogenous SOD1 gene, as well as normal nontransgenic mice.
14. A. G. Reaume *et al.*, *Nature Genet.* **13**, 43 (1996).
15. Immunoblots (70 μg of total spinal cord homogenates) were incubated with polyclonal antipeptide antibodies generated against a sequence present in human but not mouse SOD1 or against antipeptide antibodies specific for mouse SOD1 (*5*). Signals were detected with ^{125}I-labeled protein A and quantified by phosphorImaging.
16. M. C. Dal Canto and M. E. Gurney, *Acta Neuropathol.* **93**, 537 (1997).
17. M. Becher and D. L. Price, personal communication.
18. N. Shibata *et al.*, *Neurosci. Lett.* **179**, 149 (1994).
19. S. M. Chou, H. S. Wang, K. Komai, *J. Chem. Neuroanat.* **10**, 249 (1996).
20. N. Shibata, K. Asayama, A. Hirano, M. Kobayashi, *Dev. Neurosci.* **18**, 492 (1996).
21. S. M. Chou, H. S. Wang, A. Taniguchi, *J. Neurol. Sci.* **139**, 16 (1996).
22. N. Shibata *et al.*, *J. Neuropathol. Exp. Neurol.* **55**, 481 (1996).
23. S. Kato *et al.*, *ibid.*, p. 1089.
24. S. Kato *et al.*, *Am. J. Pathol.* **151**, 611 (1997).
25. C. A. Pardo *et al.*, *Proc. Natl. Acad. Sci. U.S.A.* **92**, 954 (1995).
26. S. I. Liochev, L. L. Chen, R. A. Hallewell, I. Fridovich, *Arch. Biochem. Biophys.* **346**, 263 (1997).
27. H. S. Yim, J. H. Kang, P. B. Chock, E. R. Stadtman, M. B. Yim, *J. Biol. Chem.* **272**, 8861 (1997).
28. L. Bruijn *et al.*, *Proc. Natl Acad. Sci. U.S.A.* **94**, 7606 (1997).
29. R. J. Ferrante *et al.*, *Ann. Neurol.* **42**, 326 (1997).
30. M. F. Beal *et al.*, *ibid.*, p. 646.
31. R. J. Singh *et al.*, *Proc. Natl. Acad. Sci. U.S.A.* **95**, 6675 (1998).
32. A. C. Bowling, J. B. Schulz, R. H. Brown Jr., M. F. Beal,

J. Neurochem. **61**, 2322 (1993); J. M. McCord, *Science* **266**, 1586 (1994); J. O. McNamara and I. Fridovich, *Nature* **362**, 20 (1993).
33. T. L. Williamson and D. W. Cleveland, unpublished data.
34. T. L. Williamson *et al.*, *Proc. Natl. Acad. Sci. U.S.A.* **95**, 9631 (1998).
35. Histology and immunocytochemistry were performed as described (*5*) using antibodies to glial fibrillary acidic protein (DAKO, Carpinteria, CA) or SOD1 (*5*, *25*). For restaining of sections after treatment with hemotoxylin and eosin (H&E), coverslips were removed and decolorized with 1% HCl in 70% ethanol before immunocytochemistry.
36. We are grateful to L. B. Corson for critical reading of the manuscript and to H. Hwang for her technical assistance. This work was supported by grants to D.W.C. from NIH (NS 27036) and the ALS Association. L.I.B. was supported by a postdoctoral fellowship from the Muscular Dystrophy Association. Salary support for D.W.C. is provided by the Ludwig Institute for Cancer Research. S.K. is supported by a Grant-in-Aid for Scientific Research (09680744) from the Ministry of Education, Science, Sports and Culture of Japan.

19 May 1998; accepted 28 July 1998

Regulation of Meiotic S Phase by Ime2 and a Clb5,6-Associated Kinase in *Saccharomyces cerevisiae*

Léon Dirick, Loretta Goetsch, Gustav Ammerer, Breck Byers*

Cyclin-dependent kinase (Cdk) mutations that prevent entry into the mitotic cell cycle of budding yeast fail to block meiotic DNA replication, suggesting there may be fundamental differences between these pathways. However, S phase in meiosis was found to depend on the same B-type cyclins (Clb5 and Clb6) as it does in mitosis. Meiosis differs instead in the mechanism that controls removal of the Cdk inhibitor Sic1. Destruction of Sic1 and activation of a Clb5-dependent kinase in meiotic cells required the action of the meiosis-specific protein kinase Ime2, thereby coupling early meiotic gene expression to control of DNA replication for meiosis.

In eukaryotes, both mitotic chromosomal DNA replication (S phase) and chromosome segregation (M phase) are triggered by cyclin-dependent kinases (Cdks). In budding yeast, specific B-type cyclins activate the principal Cdk, Cdc28, to control entry into S phase. Late in G_1, a series of events leads to activation of the S-phase promoting factor (SPF), a complex of Cdc28 with either of two similar B-type cyclins, Clb5 and Clb6 (*1–3*). Before S phase, the Clb5,-6/Cdc28 kinase is maintained in an inactive state by its association with the CDK inhibitor (CDI) Sic1. Targeting of Sic1 for degradation requires activity of the Cdc28 kinase in conjunction with the G_1-specific cyclins Cln1 and Cln2 (*4–7*). In mutants lacking Clb5 and Clb6, S phase occurs but is delayed, because other B-type cyclins (*CLB1–4*) that arise later in the cell cycle can also fulfill this function (*8*).

In meiosis, the G_1- to S-phase transition is controlled differently. The temperature-sensitive CDK mutation that blocks mitotic S phase, *cdc28-4*, has no effect on meiotic S phase (*9*). Thus, Cdc28 might render mitotic DNA synthesis dependent on growth conditions, while being dispensable for meiotic S phase (*10*). One possibility is that the meiosis-specific kinase encoded by *IME2*, which has sequence similarity to Cdc28 and is required for meiotic S phase (*11–13*), replaces Cdc28 in an SPF-like function that is required in meiosis. To find out, we have reinvestigated genetic interactions that influence DNA replication in meiosis.

Yeast strains mutant for the G_1-specific cyclins *CLN1,-2,-3* are blocked in mitosis at G_1 (*14*, *15*) but form viable spores to the same extent as do wild-type (WT) cells (*16*, *17*). Likewise, mutations eliminating components of transcription factors for the *CLN1* and *CLN2* genes (*SBF* and *MBF*) cause mitotic G_1 arrest (*18*) but fail to block meiosis (*16*, *17*). These findings are consistent with a differential control of S phase between mitosis and meiosis, but the results of introducing mutations in *CLB5* and *CLB6* (*19*) are not. Although a strain deleted for *CLB6* is fully proficient in sporulation, a *clb5*Δ homozygote fails to sporulate (*16*) (Fig. 1C). Because different genetic backgrounds vary in sporulation efficiency, we also tested *clb5*Δ in two other strain backgrounds (W303 and YK) and obtained similar results (*16*, *19*). Meiotic S phase (*20*) in a *clb5*Δ homozygote was delayed about 3 hours relative to the WT (Fig. 1B) and meiotic progression was blocked either in G_2 (60% of cells) or in meiosis I (40% of cells) (Fig. 1, A and C). The delay of S phase did not result from delayed initiation of meiosis, for the increase in transcription of both *IME2* (an early meiotic gene) and *CLB6* occurred on schedule and to even higher levels than that in WT cells (Fig. 1D) (*20*). Assessment of intragenic recombination within the *HIS4* locus revealed no His^+ progeny (*21*), indicating either that *CLB5* is required for recombination or that recombinants are inviable. We conclude that *CLB5* function is required for scheduled entry into S phase and that *clb5*Δ homozygotes, despite their capacity for extensive DNA replication, are unable to progress normally through subsequent stages of meiosis. These latter anomalies might reflect either qualitative defects in the newly replicated DNA or an additional requirement for *CLB5* function in the transition from G_2 to meiosis I. The finding that *CLB5* is also activated by the G_2-specific meiotic transcription factor Ndt80 (*22*) favors the latter explanation.

Because *CLB6* is functionally redundant with *CLB5* in mitosis (*1–3*), we also tested strains deleted for both genes (*16*). In both genetic backgrounds tested, sporulation failed to occur and DNA replication was impaired to a greater extent than in cells lacking *CLB5* alone (Fig. 1, B and C), which indicates that either *CLB5* or *CLB6* can act to promote meiotic DNA synthesis. Flow cytometric profiles showed late and incomplete DNA replication, and further progression through the meiotic pathway did not occur (Fig. 1, A and B) (*21*).

Because both the Clb5 and Clb6 cyclins and the Ime2 kinase are required for meiotic DNA replication (Fig. 1) (*11–13*), they might constitute a single complex that promotes the G_1-S transition in meiosis (Fig. 4B2). Alternatively, Ime2 might mediate entry into S phase indirectly by controlling removal of an inhibitor, such as Sic1 (Fig. 4B3). The target of this inhibitor would be an unspecified meiotic Cdk (designated X) that is activated by association with Clb5 and Clb6, and the role of Ime2 in meiosis would parallel that of Cln1,-2/Cdc28 in mitosis. In this case, deletion of *SIC1* might render *IME2* dispensable for DNA replication. Indeed, deletion of *SIC1* in *ime2*Δ cells restored DNA replication to the level and kinetics observed for the control *sic1*Δ strain (Fig. 2). Thus, Sic1 acts by blocking entry into meiotic S phase, and Ime2, instead of promoting entry directly, may con-

L. Dirick, L. Goetsch, B. Byers, Department of Genetics, Box 357360, University of Washington, Seattle, WA 98195–7360, USA. G. Ammerer, Department of Biochemistry and Molecular Cell Biology, Ludwig Boltzmann Institute, University of Vienna, Dr. Bohr-Gasse, 9, A-1030 Vienna, Austria.

*To whom correspondence should be addressed.